12th International Conference on Fracture Mechanics of Concrete and Concrete Structures
FraMCoS-12
B.L.A. Pichler, Ch. Hellmich, P. Preinstorfer (Eds)

https://doi.org/10.21012/FC12.1339
MS15-2:2

SELF-HEALING PROPERTIES OF SEAWATER SEA-SAND STRAIN-HARDENING CEMENTITIOUS COMPOSITES (SHCC)

JING YU[*], FENG HU[†]

[*] Department of Civil Engineering, The University of Hong Kong
Hong Kong, PR China
e-mail: ceyujing@hku.hk

[†] School of Civil Engineering, Sun Yat-Sen University
Guangzhou, PR China
e-mail: hufeng9@mail2.sysu.edu.en

Key words: Strain-Hardening Cementitious Composites (SHCC); Engineered Cementitious Composites (ECC); Seawater Sea-Sand Concrete; Self-Healing; Mechanical Properties

Abstract: Seawater sea-sand concrete reinforced with non-corrosive reinforcements is attractive for marine infrastructures, while self-healing of cracks can enhance the longevity of concrete structures under harsh marine environments. However, current knowledge on the self-healing properties of Seawater Sea-sand Strain-Hardening Cementitious Composites (SS-SHCC) remains limited. This study aims to address this gap by investigating the self-healing mechanism and multi-scale healing performance of SS-SHCC. Firstly, the self-healing mechanism of SS-SHCC was explored at a single crack level. The effects of binder composition, initial crack width, and exposed conditions (involving seawater wet-dry cycling and immersion) on the self-healing behavior of the matrix were explored. Crack width was monitored throughout the healing period, and the self-healing products were characterized using X-ray diffraction, thermogravimetric analysis, and scanning electron microscopy. Subsequently, the multi-scale self-healing performance of the SS-SHCC was evaluated across four simulated marine environments. Surface crack healing and resonant frequency measurements were assessed during self-healing, while permeability and mechanical performance tests were conducted after self-healing. The findings revealed that the primary self-healing products in marine environments consisted of portlandite, brucite, aragonite, and calcite. The self-healing performance was primarily governed by the availability of Ca^{2+} and OH^- ions precipitating from the matrix. The presence of seawater in marine environments is pivotal for the self-healing efficacy of SS-SHCC, and the self-healing of SS-SHCC in the air zone was less pronounced. With the exception of the air zone, SS-SHCC's normalized resonant frequency recovered to more than 75% of its initial value, while permeability stayed below 1×10^{-10} m/s, preserving outstanding mechanical properties. These findings provide valuable insights for the design and application of SS-SHCC, contributing to enhanced durability and longevity of marine infrastructures.

1 INTRODUCTION

Nowadays, cost-effective seawater sea-sand concrete combined with non-corrosive reinforcements are increasingly favoured for marine infrastructures [1, 2]. However, seawater sea-sand concrete fails to alter the poor ductility of ordinary concrete, and the structures become highly prone to cracking in harsh marine environments, severely limiting their service life.

Self-healing phenomenon in concrete can minimize the negative effects of cracking. This process is sensitive to crack width, and it is

generally believed that cracks in the micron scale can achieve obvious self-healing effect [3]. Therefore, it is of great interest to find a cementitious material with reliable crack control ability and self-healing potential in marine environment.

Strain-Hardening Cementitious Composites (SHCC) are a class of advanced fiber-reinforced cementitious materials featured with reliable crack control capabilities [4, 5] and self-healing potential in harsh ionic environments [6-8]. Furthermore, existing studies have demonstrated that seawater sea-sand SHCC (SS-SHCC) exhibits excellent mechanical properties [9, 10], making it an ideal material for marine infrastructures with self-healing potential. The self-healing mechanisms and multiscale self-healing behaviors of SS-SHCC under marine environments require further investigation.

2 MATERIALS AND METHODS

Specimens were prepared using CEM I 52.5R Portland cement, ASTM Class F fly ash (FA), sea sand (particle size ≤ 300 μm), polyethylene (PE) fibers, artificial seawater, and polycarboxylate superplasticizer. The water/binder ratio was fixed at 0.25. For the first phase of study, cement paste was prepared by partially replacing 25–75% of the cement with fly ash. To evaluate the self-healing performance at different curing ages, two conditions were considered: (1) standard curing for 28 days (28d) and (2) accelerated aging (aa), where specimens were cured in 60°C seawater for 5 weeks following the standard 28-day curing. Prism specimens underwent three-point bending tests until failure, after which one was divided into four pieces. Waterproof tape of varying thicknesses was applied at the corners to create controlled initial internal crack widths (150 - 450 μm). Then, the mixture with high self-healing potential and maximized fly ash dosage was selected, and sea-sand and PE fibers were incorporated to produce SS-SHCC. After 28 days of standard curing, SS-SHCC specimens were subjected to preloading under uniaxial tension (1% and 2% strain) to induce cracks. The cracked SS-SHCC specimens were then exposed to different self-healing conditions.

3 SELF-HEALING MECHANISM OF SS-SHCC

3.1 Self-healing rate of cracks

The self-healing environments were set to wet-dry cycling and seawater immersion, with a self-healing duration of 56 days. **Figure 1** shows the crack healing rates of seawater cement pastes (after 28-day or accelerated aging curing) under different self-healing exposures after 56 days. As the content of FA, initial crack width and curing age increased, the crack healing rate gradually decreased for different environments.

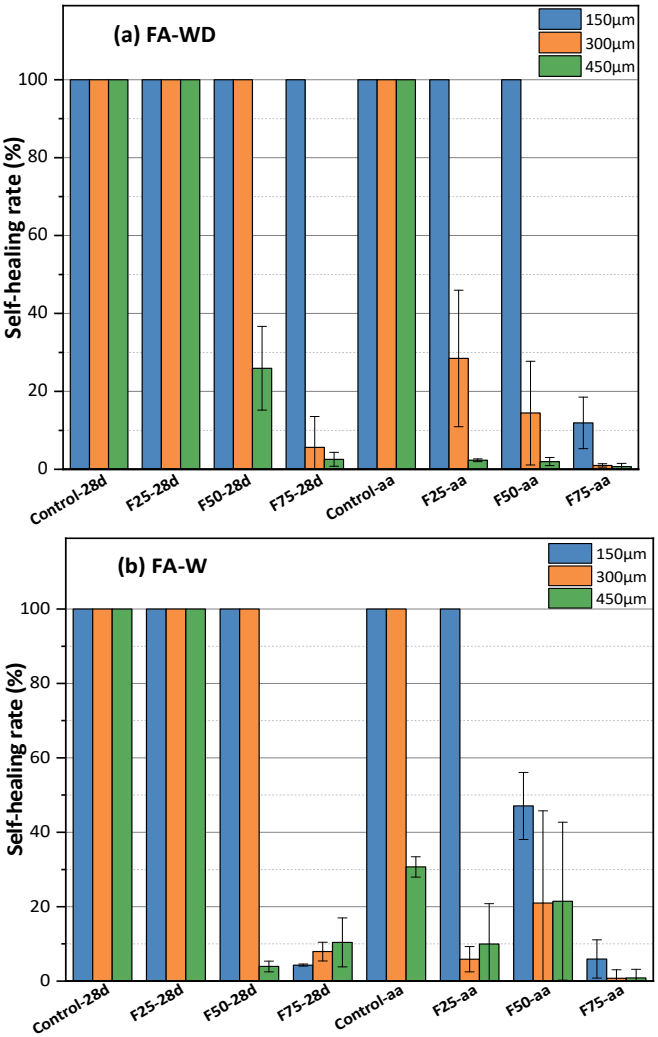

Figure 1: Crack self-healing rates for 28-day and aging specimens with different initial crack widths after 56-day exposure in: (a) Wet-dry cycling (WD); (b) Seawater immersion (W).

3.2 Self-healing products in cracks

Figure 2 displays the X-ray diffraction (XRD) results of self-healing products generated in the crack width of 150 μm. The main self-healing products are portlandite (#44-1481), brucite (#44-1482), aragonite (#41-1475), and calcite (#47-1743) [11, 12].

Figure 3 shows the thermogravimetric analysis (TGA) results of the self-healing products. The mass loss in the temperature range of 350-420℃ was attributed to the decomposition of $Mg(OH)_2$ [11], the mass loss around 450℃ was attributed to the decomposition of $Ca(OH)_2$, and the loss between 600-900℃ was attributed to the decomposition of $CaCO_3$ [13].

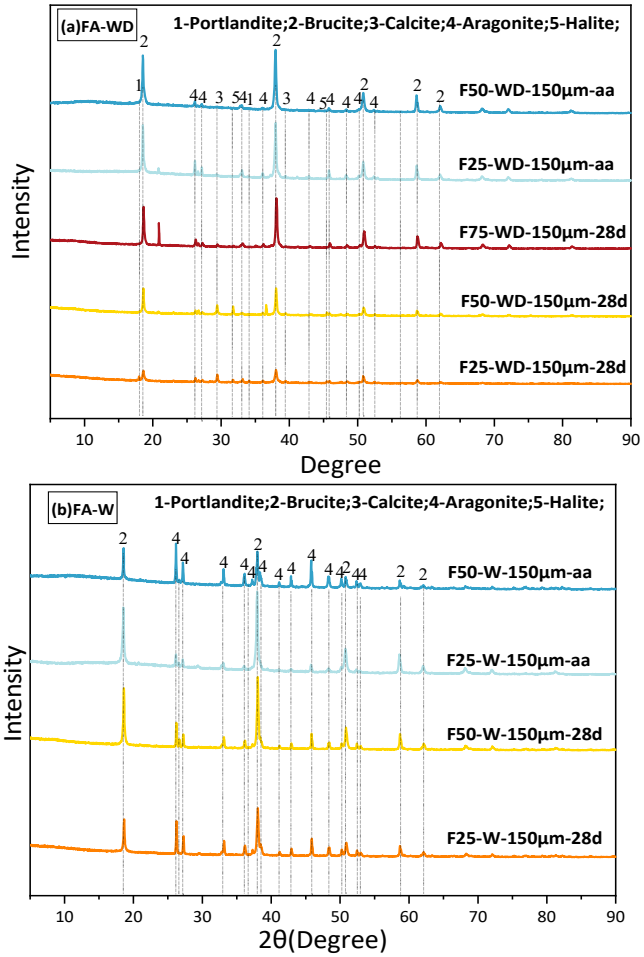

Figure 2: XRD of self-healing products in 150 μm cracks: (a) Wet-dry cycling; (b) Seawater immersion.

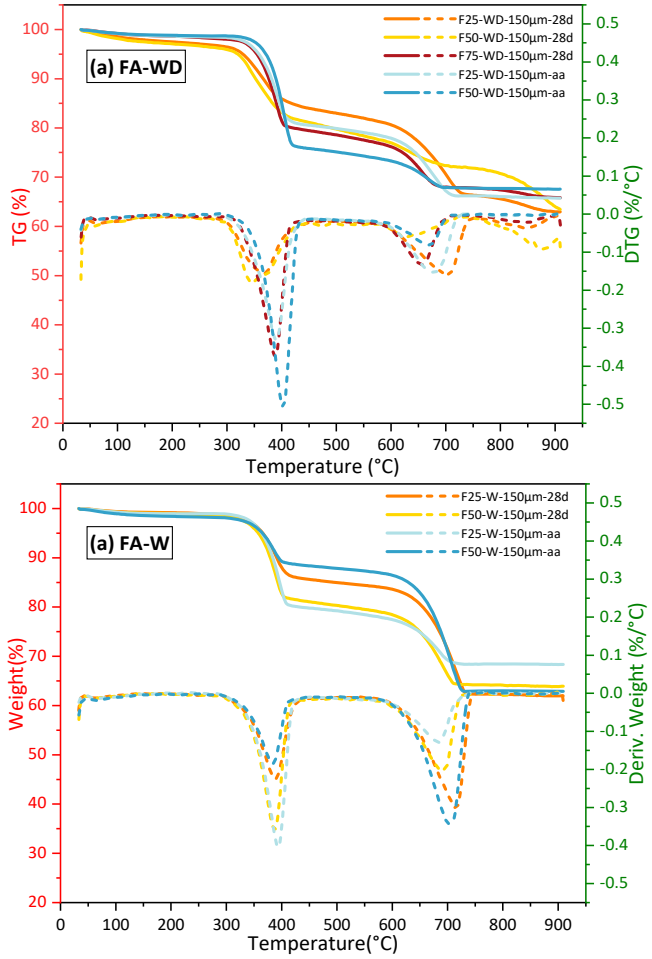

Figure 3: TG of self-healing products in 150 μm cracks: (a) Wet-dry cycling; (b) Seawater immersion.

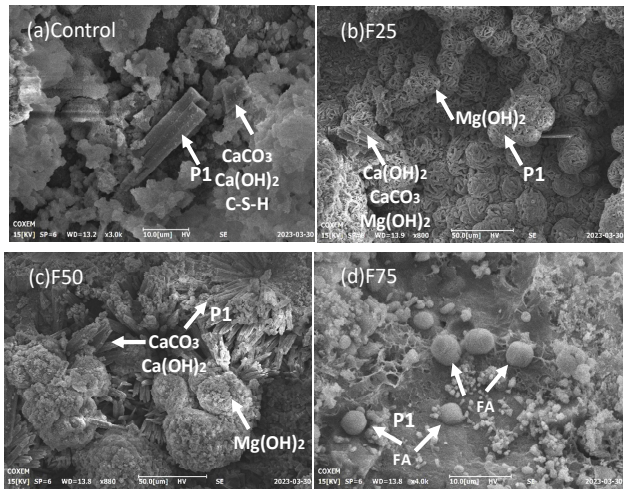

Figure 4: SEM images of 150-μm cracks.

Figure 4 presents the SEM images of cracks under seawater immersion. The main self-healing products in the seawater environment were $Ca(OH)_2$, $Mg(OH)_2$, and $CaCO_3$. Very limited self-healing products

were observed in the crack of the F75 specimens, and the un-hydrated and hydrating FA particles remained present (**Figure 4**d).

4 MULTI-SCALE SELF-HEALING PERFORMANCE OF SS-SHCC

4.1 Self-healing progress of surface cracks

Based on the findings of the first phase of study, the fly ash replacement ratio in SS-SHCC was set at 50%. This mix proportion was further investigated to explore the multi-scale self-healing performance of SS-SHCC. Self-healing was evaluated under four simulated marine environments: (A) Air zone, (T) Tidal zone, (S) Splash zone, and (W) Immersion zone, with a self-healing period of 20 days. **Figure 5** displays surface images of SS-SHCC cracks. Specimens in the air zone showed no significant crack closure during the self-healing period, while surface cracks in the tidal and submerged zones healed rapidly. Meanwhile, the healing products were uniformly and continuously deposited within cracks.

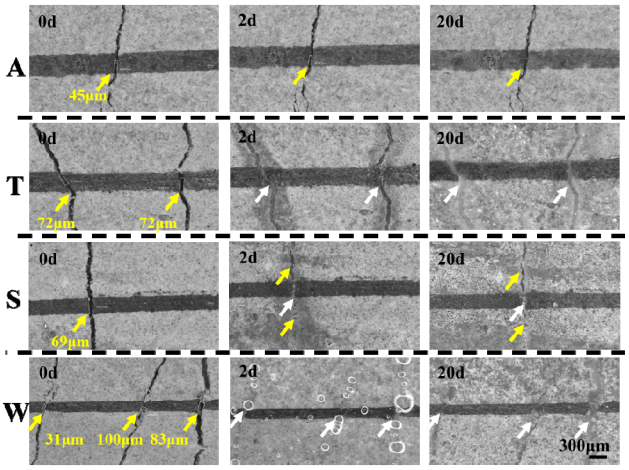

Figure 5: Crack photos during self-healing in different environments: (A) Air zone; (T) Tidal zone; (S) Splash zone; (W) Immersion zone.

4.2 Resonant frequency

The normalized resonant frequency (RF) test results are depicted in **Figure 6**. After 20 days of self-healing in the four marine environments, except for the air zone, the normalized RF recovery ratio for specimens with 1% and 2% preloading reached 90% and 75%, respectively. In seawater-exposed environments, 20 days of self-healing effectively restored the resonant frequency, which aligned with the observed trend of surface crack closure.

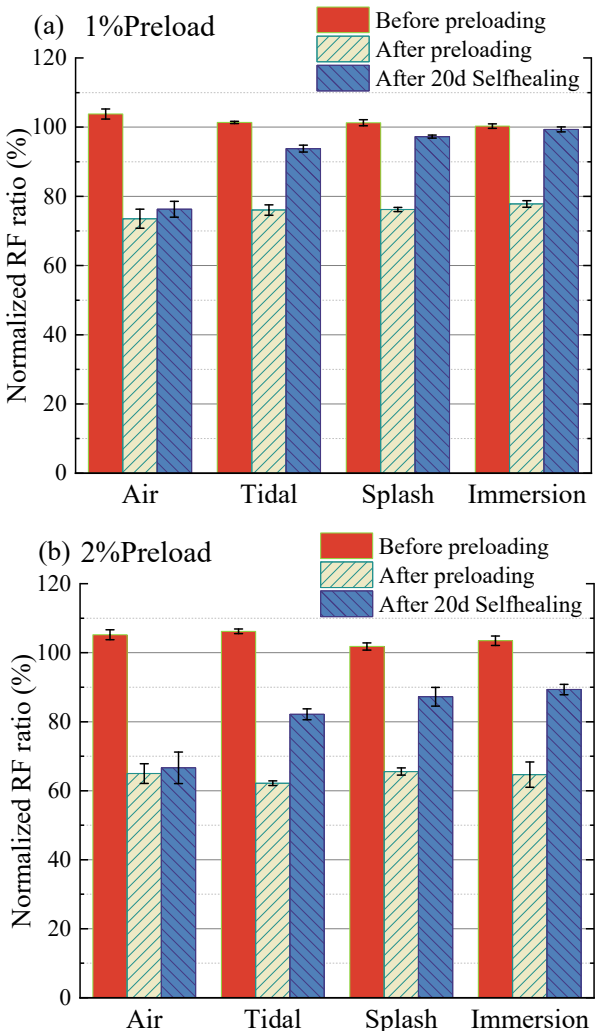

Figure 6: Normalized resonance frequency recovery ratio: (a) SHCC-1% Preload; (b) SHCC-2% Preload.

4.3 Water permeability

The water permeability of uncracked and healed SS-SHCC specimens is shown in **Figure 7**. The durability of marine concrete structures is primarily governed by their impermeability, as seawater-induced deterioration typically initiates through transport pores. Therefore, impermeability plays a crucial role in ensuring long-term structural durability. After 20-day self-healing, the water permeability coefficient of SS-SHCC under varying preloading strains

recovered to below 1×10^{-10} m/s, reinforcing excellent self-healing performance in seawater environments.

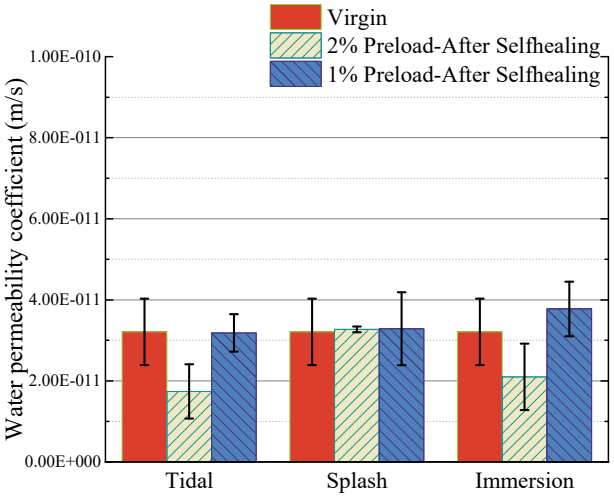

Figure 7: Water permeability coefficient of SS-SHCC after self-healing.

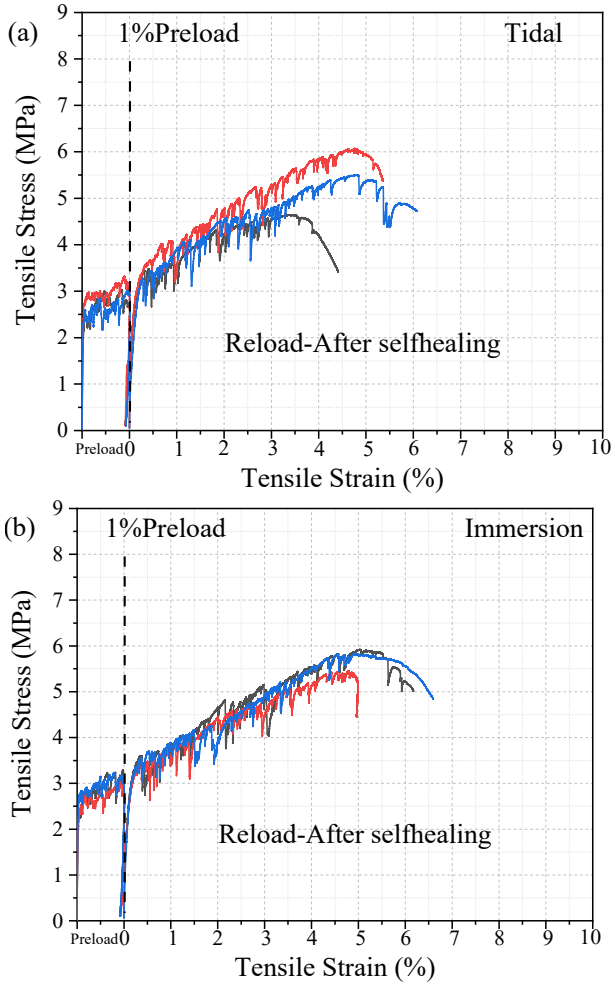

Figure 8: Uniaxial tensile test after self-healing (1% pre-load): (a) Tidal zone; (b) Immersion zone.

4.4 Uniaxial tensile behavior

After 20-day self-healing, uniaxial tensile tests were performed on the healed specimens (**Figure 8**). The SS-SHCC specimens healed in the tidal zone and immersion zone exhibited significant strain-hardening characteristics under reloading, with uniaxial tensile strain exceeding 5%.

4.5 Self-healing products in SS-SHCC

The crack surfaces of SS-SHCC after tensile failure are shown in **Figure 9**. The primary self-healing products observed on the crack surfaces were $Ca(OH)_2$ and $CaCO_3$. These healing products were predominantly deposited along the crack interfaces, whereas no significant deposition was found on the PE fibers. Additionally, un-hydrated fly ash particles undergoing hydration were observed on the crack surfaces, as shown in **Figure 9**b.

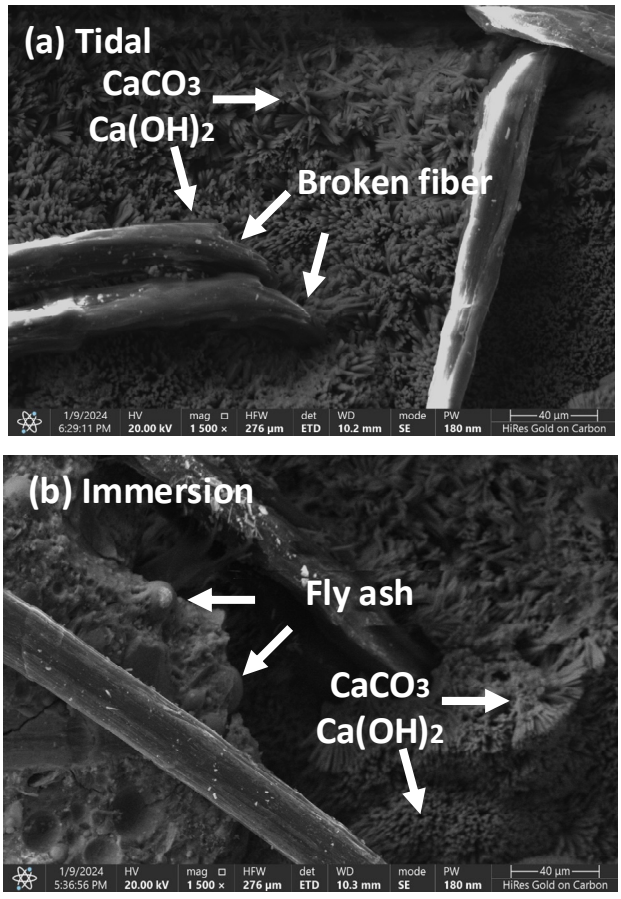

Figure 9: Microstructure of matrix-fiber after reloading: (a) Tidal zone; (b) Immersion zone.

5 CONCLUSIONS

This study investigated the self-healing mechanism and multi-scale healing performance of Seawater Sea-sand Strain-Hardening Cementitious Composites (SS-SHCC). Major conclusions are:

(1) The main self-healing products include portlandite, brucite, aragonite and calcite in marine environments.
(2) Exposure to seawater in marine environments plays a vital role in achieving effective self-healing.
(3) The self-healing recovery in SS-SHCC is most pronounced within the initial 2 days, with substantial crack closure occurring during this period.
(4) Except in the air zone, the normalized RF of SS-SHCC recovered to over 75% of its initial value, while the permeability coefficient remained less than 1×10^{-10} m/s, maintaining excellent mechanical performance.

ACKNOWLEDGEMENT

National Natural Science Foundation of China (52108264).

REFERENCES

[1] J.G. Teng, T. Yu, J.G. Dai, G.M. Chen, FRP composites in new construction: current status and opportunities, *The 7th National Conference on FRP Composition in Infrastructure*, Hangzhou, China, 2011.

[2] X. Hu, T. Bai, Y. Zhao, Q. Ren, Y. Chen, H. Li, C. Shi, Interface mechanical properties of CFRP-seawater sea sand concrete under simulated seawater immersion, *Journal of Building Engineering* 97 (2024) 110768.

[3] E.-H. Yang, Designing Added Functions in Engineered Cementitious Composites, *PhD Thesis*, University of Michgan, USA, 2008.

[4] S. Qudah, M. Maalej, Application of Engineered Cementitious Composites (ECC) in interior beam–column connections for enhanced seismic resistance, *Engineering Structures* 69 (2014) 235-245.

[5] J. Ji, Z.-B. Zhang, M.-F. Lin, L.-Z. Li, L.-Q. Jiang, Y. Ding, K.-Q. Yu, Structural application of engineered cementitious composites (ECC): A state-of-the-art review, *Construction and Building Materials* 406 (2023) 133289.

[6] H.-L. Wu, Y.-J. Du, J. Yu, Y.-L. Yang, V.C. Li, Hydraulic conductivity and self-healing performance of Engineered Cementitious Composites exposed to Acid Mine Drainage, *Science of The Total Environment* 716 (2020) 137095.

[7] J.-S. Qiu, H.-S. Tan, E.-H. Yang, Coupled effects of crack width, slag content, and conditioning alkalinity on autogenous healing of engineered cementitious composites, *Cement and Concrete Composites* 73 (2016) 203-212.

[8] H.-Z. Liu, Q. Zhang, C.-S. Gu, H.-Z. Su, V.C. Li, Self-healing of microcracks in Engineered Cementitious Composites under sulfate and chloride environment, *Construction and Building Materials* 153 (2017) 948-956.

[9] B.-T. Huang, J. Yu, J.-Q. Wu, J.-G. Dai, C.K. Leung, Seawater sea-sand Engineered Cementitious Composites (SS-ECC) for marine and coastal applications, *Composites Communications* 20 (2020) 100353.

[10] J.-T. Yu, K.-K. Liu, Q.-F. Xu, Z.-H. Li, L.-J. Ouyang, Feasibility of using seawater to produce ultra-high ductile cementitious composite for construction without steel reinforcement, *Structural Concrete* 20(2) (2019) 774-785.

[11] H. Liu, H.-L. Huang, X.-T. Wu, H.-X. Peng, Z.-H. Li, J. Hu, Q.-J. Yu, Effects of external multi-ions and wet-dry cycles in a marine environment on autogenous self-healing of cracks in cement paste, *Cement and Concrete Research* 120 (2019) 198-206.

[12] D. Palin, V. Wiktor, H.M. Jonkers, Autogenous healing of marine exposed concrete: Characterization and quantification through visual crack closure, *Cement and Concrete Research* 73 (2015) 17-24.

[13] X.-T. Wu, H.-L. Huang, H. Liu, Z.-F. Zeng, H.-D. Li, J. Hu, J.-X. Wei, Q.-J. Yu, Artificial aggregates for self-healing of cement paste and chemical binding of aggressive ions from sea water, *Compos Part B-Eng* 182 (2020) 107605.